The riverine flux of molybdenum and its isotopes to the ocean: Weathering processes and dissolved-particulate partitioning in the Amazon basin

Author(s):
Revels, Brandi N.; Rickli, Jörg; Moura, Candido A.V.; Vance, Derek

Publication date:
2021-04-01

Permanent link:
https://doi.org/10.3929/ethz-b-000467219

Originally published in:
Earth and Planetary Science Letters 559, https://doi.org/10.1016/j.epsl.2021.116773

Funding acknowledgement:
165904 - Metal isotope constraints on biosphere-environment interactions in Earth history (SNF)

Earth and Planetary Science Letters 559 (2021) 116773

Contents lists available at ScienceDirect

Earth and Planetary Science Letters

www.elsevier.com/locate/epsl

The riverine flux of molybdenum and its isotopes to the ocean: Weathering processes and dissolved-particulate partitioning in the Amazon basin

Brandi N. Revels [a], Jörg Rickli [a], Candido A.V. Moura [b], Derek Vance [a,*]

[a] Department of Earth Sciences, ETH Zürich, Clausiusstrasse 25, 8092 Zürich, Switzerland
[b] Universidade Federal do Pará, Instituto de Geociências, Rua Augusto Correa, 1-66075-110, Belém-PA, Brazil

ARTICLE INFO

Article history:
Received 11 November 2020
Received in revised form 14 January 2021
Accepted 19 January 2021
Available online xxxx
Editor: F. Moynier

Keywords:
molybdenum
isotopes
chemical weathering
Amazon
riverine flux
ocean

ABSTRACT

Molybdenum (Mo) abundances and isotopes in marine sedimentary rocks have become important tools for understanding the past redox state of the ocean-atmosphere system. Their use depends critically on the size and isotope composition of the dissolved riverine input to the oceans. Previous studies have demonstrated that rivers are isotopically heavier than the upper continental crust, but the reasons why are debated. The debate is important to the question of how the riverine input might change through Earth history, for example in response to tectonic- and climate-driven changes in weathering regime. Here, we present a comprehensive study of Mo and its isotopes in multiple tributaries of the Amazon Basin, across seasons, with the aim of understanding both the controls on riverine transport of Mo and its isotopes and the input to the oceans.

For all Amazonian rivers, the dissolved load dominates over the particulate load for Mo, whether the size of the total suspended load is quantified by *in-situ* filtration or from approaches using cosmogenic data. This finding is common to other highly soluble elements like strontium (Sr), and is very different from published compilations of global rivers, where particulate/dissolved ratios of Mo and Sr have been reported to be an order of magnitude higher than found here for the Amazon. Mo isotope data for the dissolved phase (<0.45 μm) of Amazon rivers (δ^{98}Mo = +0.52 to +1.46, relative to SRM NIST 3134 = +0.25) show substantially less variation than rivers globally (−0.2 to +2.4‰), but Mo concentrations vary over two orders of magnitude (0.06-6.2 nmol kg^{-1}). There is systematic variability between river types, with black and clear water rivers like the Negro and the Tapajós-Trombetas having much lower concentrations and higher Mo isotope ratios than white water rivers. Low water season (November) concentrations are always greater, and Mo isotope compositions lighter, than high water season (June). A small number of analyses shows that the colloidal phase (<0.45 μm, 1 kDa) represents about 20-30% of the total dissolved load, is broadly similar in isotope composition, and invariant in size between seasons. Thus, the greater dissolved concentration and lighter isotope composition in November must predominantly be driven by changes in the "truly-dissolved" fraction.

We find little evidence for lithological or mineralogical controls on the Mo isotope composition of Amazonian rivers. Dissolved Mo concentrations are well-correlated with other highly soluble elements found in major minerals, be they silicates, carbonates or sulphides. Rather, molybdenum isotope variations across tributaries and season are best explained by processes related to the weathering regime, including preferential mobilisation of heavy isotopes due to sequestration of the light isotopes to secondary phases in soils. In more detail, soil pH is suggested to play a secondary, but significant, role. The assessment of the global dataset for Mo in rivers in terms of these processes suggests that there could be significant temporal variability in the riverine source of Mo to the oceans, controlled by tectonics and climate and their impact on weathering regime.

1. Introduction

The removal of molybdenum and its isotopes from the dissolved pool of the ocean, and their partitioning between different sedi-

* Corresponding author.
E-mail address: derek.vance@erdw.ethz.ch (D. Vance).

https://doi.org/10.1016/j.epsl.2021.116773

mentary sinks, holds information on the past redox state of the ocean-atmosphere system (for a recent review, see Kendall et al., 2017). The approach relies on the redox-dependence of Mo speciation in the ocean, the contrasting solubilities of these different species, and isotope fractionations that stable Mo isotopes undergo during speciation changes and removal to particulates.

In oxidizing marine environments, the main output flux is slow adsorption onto Mn-oxyhydroxides, which are fractionated from seawater by $-3‰$ (Siebert et al., 2003; Barling and Anbar, 2004; Wasylenki et al., 2008: Mo isotope compositions throughout the paper are given as parts per thousand deviations of the $^{98}Mo/^{95}Mo$ ratio, $\delta^{98}Mo$, from NIST SRM3134 $= +0.25‰$; Nägler et al., 2014). This light output is the main driver of the heavy isotopic composition of Mo in modern seawater relative to the inputs (Siebert et al., 2003; Archer and Vance, 2008; Nakagawa et al., 2012). On the other hand, Mo is rapidly removed in sulfidic environments, due to the transformation of soluble molybdate to particle-reactive thiomolybdates ($MoO_{4-x}S_x^{2-}$, $1 < x < 4$: Helz et al., 1996). In strongly euxinic settings, this transformation is nearly complete, sediments are enriched in Mo (Morford and Emerson, 1999), and can have isotope compositions that approach seawater (Nägler et al., 2005; Neubert et al., 2008). The most important sedimentary sink is, however, open marine upwelling margins (e.g. Kendall et al., 2017). The sediments of such settings feature a wide range of $\delta^{98}Mo$ that are isotopically intermediate between the light oxic sink and modern seawater (e.g. Siebert et al., 2006; Poulson Brucker et al., 2009), driven by multiple Mo fixation mechanisms.

The application of sedimentary Mo and its isotopes to the investigation of the mass balance of oceanic sinks, and the record of redox in the ancient ocean that this holds, relies on a sound understanding of the source fluxes to the oceans. The early assumption (e.g. Arnold et al., 2004) was that the main input flux to the oceans derived from the dissolved load of rivers, and that this source is isotopically identical to igneous rocks of the upper continental crust (UCC) at 0 to $+0.3‰$ (see Kendall et al., 2017). Archer and Vance (2008) first showed that the Mo dissolved in rivers is often substantially heavier than the UCC. Subsequent studies have confirmed this finding (Pearce et al., 2010: Neubert et al., 2011; Voegelin et al., 2012; Rahaman et al., 2014; Wang et al., 2015; King and Pett-Ridge, 2018; Neely et al., 2018; Horan et al., 2020), and report riverine Mo isotope compositions up to the value of the oceans. Archer and Vance (2008) noted a systematic relationship between riverine $\delta^{98}Mo$ and Mo concentrations, with high concentrations associated with lighter Mo isotopes close to igneous rocks, and progressively heavier values associated with decreasing concentrations. These authors suggested that this relationship was caused by the sequestration of light Mo isotopes to secondary mineral phases in the weathering environment and the preferential release of heavy Mo isotopes to the dissolved phase, a conclusion also arrived at in other studies of rivers (e.g. Pearce et al., 2010; Wang et al., 2015; Horan et al., 2020). Subsequent soil studies have confirmed that light isotopes are retained in soils, perhaps by soil organic matter in addition to secondary minerals (e.g. Siebert et al., 2015; King et al., 2016, 2018; Wang et al., 2018).

In contrast to this view, another group of studies of both global Mo abundance patterns in rivers (Miller et al., 2011) and Mo isotope studies of small river catchments (Neubert et al., 2011; Voegelin et al., 2012) have placed a much greater emphasis on catchment lithology, in particular the preferential chemical weathering of isotopically heavy sulphide and sulphate minerals. In addition to this debate over the precise controls on Mo and its isotopes in the dissolved load itself, recent compilations of dissolved and particulate data for global rivers have suggested that the particulate load of Mo is about 3 times larger than the dissolved load (Viers et al., 2009). The data from this compilation have been used to suggest that this particulate load may actually be a significant oceanic input source for many elements including Mo, if this material is remobilised in estuaries and continental margins (e.g. Oelkers et al., 2011; Jeandel and Oelkers, 2015).

The detailed lithological and mineralogical controls on Mo in rivers, its response to different weathering regimes, and the relative size of dissolved and particulate riverine loads, all represent uncertainties regarding the nature of the riverine source of Mo that potentially complicate the interpretation of ancient sedimentary Mo isotope data. Here we present the results of a detailed study of the abundance and isotope composition of Mo in carrier phases (dissolved, particulate, colloidal) of the Amazon River and its major tributaries, across seasons. The different weathering regimes and river chemistries of the Amazon and its tributaries allow us to shed light on the processes controlling Mo in the weathering environment. We also set the data in a global context, attempting to extract general information on the controls on Mo delivery to the oceans by rivers.

2. The Amazon basin and its rivers

The Amazon Basin (Fig. 1) drains an area of 6.1×10^6 km^2 and covers ~5% of the Earth's land surface. The Amazon River is responsible for 15-18% of global water and 6% of suspended sediment discharge to the ocean (Callède et al., 2010). Importantly for this study, the different tributaries in the basin allow us to explore the behaviour of Mo and its isotopes in different riverine systems, and how they vary with weathering regime and river chemistries.

The major tributaries of the Amazon are often classified as 'white water,' 'black water,' or 'clear water' rivers, on the basis of their colour and physicochemical characteristics (e.g. Stallard and Edmond, 1983). The Solimões and Madeira, archetypal white water rivers, drain the Andean Basin from the west. They are characterized by high discharge and exceptionally high concentrations of suspended sediments (e.g. Gaillardet et al., 1997) resulting from the erosion of newly exposed, tectonically active Andean slopes. The white water rivers are known as 'weathering limited' or 'kinetically limited' (Stallard and Edmond, 1983; West et al., 2005) because kinetic parameters such as temperature and moisture, rather than substrate supply, limit chemical weathering rates in these catchments. Limited weathering of source materials is reflected in the abundance of primary minerals such as feldspar and mica in the suspended load, and clay minerals dominated by chlorite and smectite (Gibbs, 1967). As demonstrated by Stallard and Edmond (1983), these rivers are also characterised by high alkalinity, near neutral pH, and high total cation charge ($TZ^+ > 300$ µeq/L).

In contrast to the white water rivers, the archetypal black water river, the Rio Negro, flows from the northwest lowland region of the basin and drains deeply weathered Cenozoic sediments of fluvial-lacustrine origin (Fittkau et al., 1975). Black water rivers have been described as 'transport limited' or 'supply limited' (e.g. Stallard and Edmond, 1983) because weathering rates are limited by the supply of new material to the weathering zone. These intensely weathered source regions give rise to river waters which, like their soils, are organic and humic substance rich, depleted in major cations, and enriched in refractory Si and Al as well as metals such as Fe and Zn (e.g. Gibbs, 1977; Konhauser et al., 1994; Gaillardet et al., 1997; Seyler and Boaventura, 2003), held in solution by organo-metallic complexes (Gaillardet et al., 1997; Seyler and Boaventura, 2003; Allard et al., 2011; Fritsch et al., 2011). The Negro waters have characteristically low pH and low suspended sediment concentrations (e.g. Stallard and Edmond, 1983).

The third category, 'clear water' rivers, are represented by the Trombetas and Tapajós, flowing from the north and south of the basin, respectively. The highly weathered, transport limited, stable cratonic shields give rise to the well-drained, nutrient-poor, lateritic soils rich in kaolinite, with traces of illite and smectite

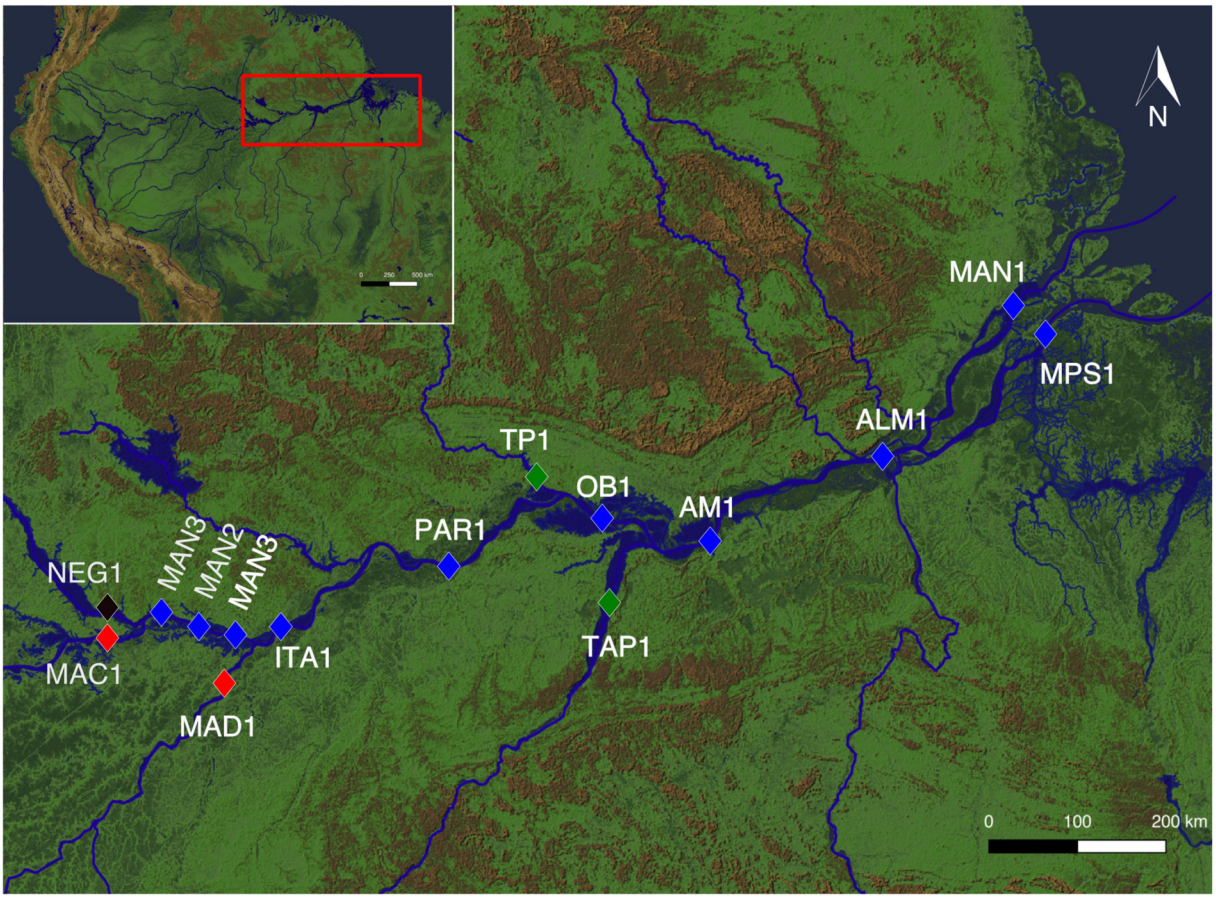

Fig. 1. Sampling locations for Amazon rivers (diamonds, with colours denoting different river chemistries as in the legends to Figs. 3–6). Background colours on the map show topography, with dark green to light brown representing low to high elevation. Sampling took place in June and November 2015 for all except stations MPN and MPS, which were only sampled in November. Additional sampling at Óbidos was done in August 2015 and January 2016. Map made with QGIS (http://qgis.osgeo.org). (For interpretation of the colours in the figure(s), the reader is referred to the web version of this article.)

(Konhauser et al., 1994). Accordingly, these rivers have characteristically low concentrations of suspended solids, near-neutral pH, and slightly higher concentrations of major cations, but with lower concentrations of Fe, Al, and Ti, than the Negro. In contrast to the Negro, however, the lack of water inundation and humic soil layers means that the clear water rivers do not have high concentrations of organic and humic compounds (Stallard and Edmond, 1983).

Lithologically, the Andean white water river catchments (Solimões and Madeira) are underlain by Paleozoic to Cenozoic sedimentary rocks, including black shales and minor evaporites, with a significant proportion of andesites, while the black and clear water catchments are dominated by intermediate to acidic igneous and metamorphic rocks of the Precambrian Guyana and Brazilian Shields (Stallard and Edmond, 1983; Gaillardet et al., 1997; Dellinger et al., 2015).

Seasonal variation in discharge of some of the main Amazon rivers is shown in Fig. 2. Sampling in this study (red arrows), covered the high and low water seasons. The percentage of the total Amazon water discharge represented by the two main white water rivers (the Solimões and Madeira) is about 73%, that of the main black water river (Negro) about 6%, and that of the main clear water rivers (Tapajós, Trombetas, Xingu) about 11% (from Gaillardet et al., 1997).

3. Methods

We have recently described the methods for sampling and filtration in some detail (Revels et al., 2021), and only a brief summary is given here. All water samples (Fig. 1) were collected from the middle of the river by boat using a pre-contaminated polycarbonate water sampler (Aquatic Research Instruments) and fitted with a Teflon-coated weight. Temperature and pH (VWR pH110 handheld meter) and alkalinity (June sampling: Macherey Nagel VISOCOLR ECO with a resolution of 5 mg/L $CaCO_3$, November: HachAL-DT with a resolution of 0.05 mg/L $CaCO_3$) were measured immediately on collection. Water for additional filtration and analysis was transferred to a clean and pre-contaminated 25 L carboy. Filtration to separate dissolved and particulate loads was done with two different methods. All <0.45 µm samples were obtained by conventional membrane filtration and, for ease of reference, these samples are referred to in the text as "dissolved". Larger volumes of water were processed to obtain particulate samples, and were filtered with a 0.45 µm cross flow filtration cartridge. We also present Mo concentration data and limited isotope data for a "colloidal" (<0.45 µm and >1 kDa) fraction obtained by cross-flow filtration of the <0.45 µm sample, from either the membrane or the cartridge approach.

All analytical work was carried out under trace metal clean conditions with distilled reagents. Aqueous samples were evaporated to dryness and the residue treated with a mixture of 1:10 peroxide and nitric acid to oxidize organic matter. Following redissolution in the same reagent, aliquots were taken for concentration and isotope analysis. The suspended sediments were subjected to a sequential extraction scheme as described in Revels et al. (2021). The extractions aimed to isolate different operationally-defined fractions, including a "residual" accessible only via attack with concentrated hydrofluoric acid and likely to be dominated

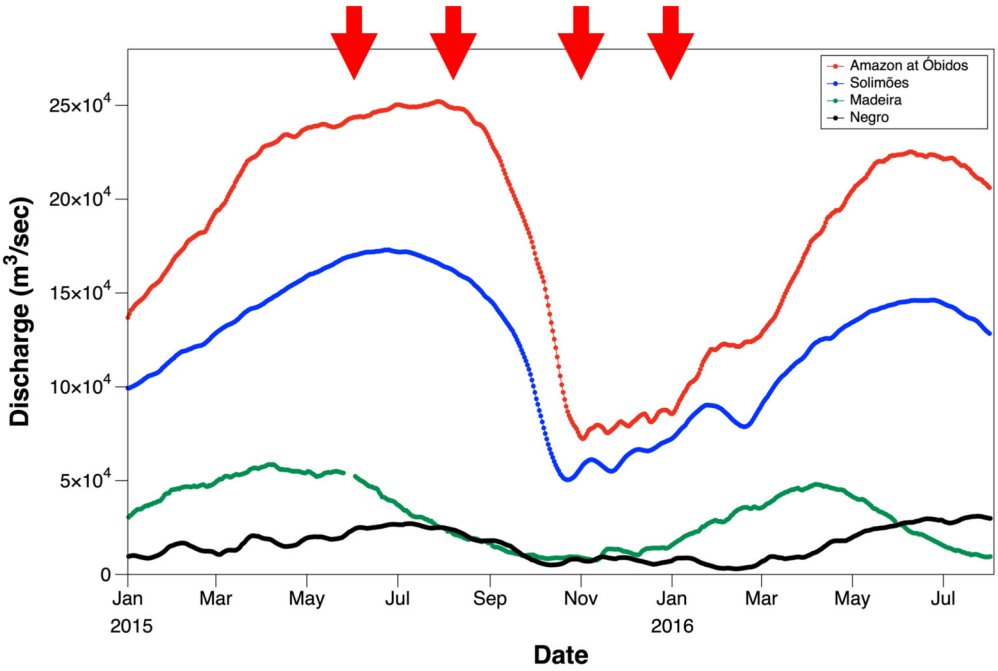

Fig. 2. Data for the discharge of Amazon rivers (from SO HYBAM, www.orehybam.org) corresponding to the following stations: the main Amazon stem at Óbidos, Solimões at Manacapuru, Madeira at Fz. Vista Alegre, Negro at Serrinha. B. Red arrows at top show the sampling times in June and November for most samples, but also August and January at Óbidos.

by primary silicate minerals. Additionally, bulk digests were analysed for some samples. Here, we report concentrations only for the residual and, where available, bulk digests, because other particulate fractions (surface adsorbed, carbonate, Fe-Mn oxyhydroxides and organic matter) proved to be too small for Mo analysis.

A small aliquot of each sample was taken for multi-element concentration analysis using a Thermo-Fisher Element XR ICP-MS at ETH Zürich (Revels et al., 2021). Precision and accuracy were assessed using two secondary standards: National Research Council of Canada river standard SLRS5, and the USGS shale standard SGR1. Accuracy was 5-20% for most elements of interest in SGR1, and 5-10% for most elements of interest in SLRS5. Precision for individual elements is typically about 10-15%. Dissolved anions (Cl^-, SO_4^{2-}, NO_3^-, F^-), dissolved organic carbon (DOC), and water isotopes (δ^2H, $\delta^{18}O$) were measured from aliquots of the 0.45 µm filtered samples.

After concentration analysis, an aliquot of sample was taken for purification of Mo, following addition of a ^{97}Mo-^{100}Mo double spike, using AG MP-1 resin (Bio-Rad) via methods previously described in Archer and Vance (2008). However, during the present study we found that newer batches of this resin had high Mo blank, so that we switched to a column involving RE-resin, as described in Bura-Nakić et al. (2018). Total procedural blanks were less than 100 pg for Mo and are negligible for all reported data. Isotopic analysis was performed on a Thermo-Finnigan Neptune multi-collector ICP-MS at ETH Zürich, following methods previously described (Bura-Nakić et al., 2018). All measurements were made relative to a zero per mil primary Elemental Scientific ICPMS (CPI) standard with standard/spike ratios in the range of 0.5-2. Relative to this standard, SRM NIST 3134 yields a value of $\delta^{98}Mo = +0.27 \pm 0.04$‰ (2SD, $n = 117$) over the past 5 years. Three full duplicate Mo isotope analyses of the dissolved fraction also reproduce at this level. All $\delta^{98}Mo$ data in this paper are presented in the standard delta notation relative to SRM NIST 3134 = +0.25‰ (Nägler et al., 2014).

4. Results

Physical, chemical, and Mo isotopic data for all of the <0.45 µm filtered samples ("dissolved") are presented in Table S1, colloidal data (<0.45 µm, >1 kDa) in Table S2, and concentration data for particulate samples in Table S3.

Molybdenum concentrations in the dissolved load vary over two orders of magnitude, with the lowest found in the Negro in June (0.06 nM) and the highest in the Madeira in November (6.2 nM). Concentrations for all rivers are higher in November than in June, by factors of up to 7. Molybdenum concentrations are tightly correlated with those of sodium (Na), across all river types and seasons (Fig. 3A). They are also strongly correlated with the concentrations of other alkalis and alkaline earths (not shown), but for these other species the relationship separates the overall dataset into two seasons, with all November data lying on a steeper correlation than those for June. This feature is summarised in the relationship between Mo concentrations versus total base cation charge (TZ^+; Fig. 3C), a parameter that has traditionally been used to separate Amazonian river types (e.g. Stallard and Edmond, 1983). Mo concentrations found in the Amazon Basin overlap with those for other major world rivers at the high end (e.g. Archer and Vance, 2008; Neubert et al., 2011; Wang et al., 2015; Horan et al., 2020), but they also extend to the much lower values found for small streams on the Hawaiian Islands (King and Pett-Ridge, 2018).

In the context of published data for rivers globally, Mo isotopes in the dissolved phase of Amazon rivers show less variation than concentrations. There is again a relationship with Na concentrations (Fig. 3B), and again the relationship with TZ^+ (Fig. 3D) separates the data by season, though less clearly than for concentrations. Consistently low $\delta^{98}Mo$ (mostly around +0.6 to +0.7‰) are found for the samples with the highest Na concentration: white water rivers and the main stem in November. The lightest isotope composition (+0.5‰) is obtained for the Óbidos sample later in the low water season (January). Significantly, the only other data we are aware of for the Amazon is for the Solimões, even later in the dry season (March, +0.6‰; Archer and Vance, 2008). The $\delta^{98}Mo$ in white water rivers and the main stem in June are higher

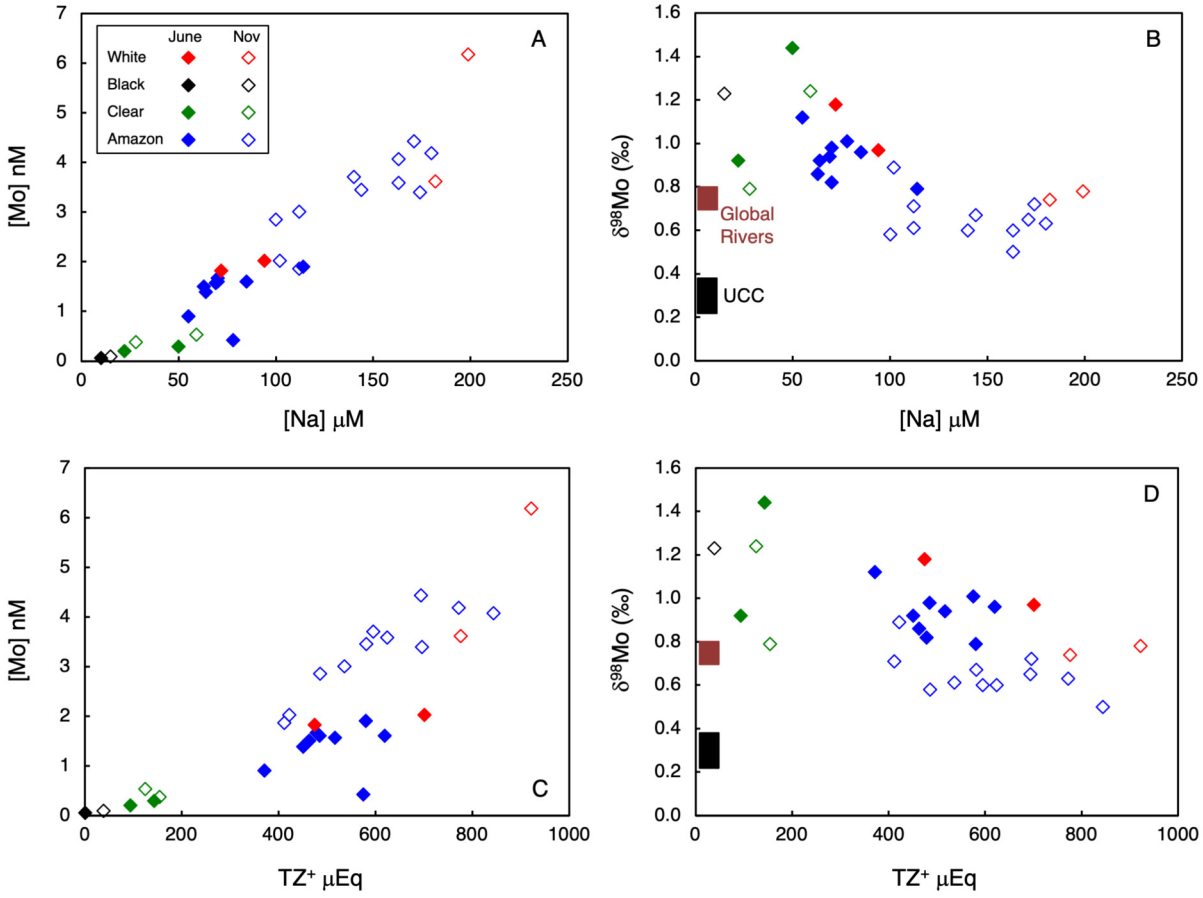

Fig. 3. Molybdenum concentrations (A, C) and Mo isotopes (B, D) versus sodium (Na) concentrations and total base cation charge ([Na] + [K] + 2[Ca] + 2[Mg]). In this and subsequent figures, the black rectangle at the left of the isotope plots gives the latest estimate of the upper continental crust (UCC) and the brown rectangle the current best estimate for the global riverine dissolved load. A value of +0.7‰ is obtained from the discharge- and Mo-concentration weighted published data for large rivers, but this is dominated by the Amazon itself. A value of +0.8‰ is more consistent with the data in this paper (seasonally-weighted Óbidos data, using hydrographic data as in Fig. 2, and Mo abundance as measured here).

than in November, mostly at +0.9 to +1.1‰. One of the clear water rivers, the Tapajós, is similar to white waters in terms of δ^{98}Mo. The Trombetas, however, shows the heaviest δ^{98}Mo of all, at +1.4‰ in June and +1.2‰ in November. Only one Mo isotope analysis was possible for the very Mo-depleted Negro, and this value is similarly heavy.

The colloidal data (Table S2) demonstrate that, in most cases, this fraction represents about 10-30% of the total dissolved load. The exception to this is the Itacoatiara (ITA) sample collected in June, where the colloidal fraction represents 80% of the total dissolved load. In principle, this could reflect an analytical issue given the low total dissolved phase Mo concentrations for this sample, but the same low value is found for an ICP-MS (Element) analysis and two MC-ICP-MS (Neptune) analyses. The sample is from directly downstream of the Madeira confluence, and it is possible that some non-conservative removal of Mo occurs here. Concentration data are available for both June and November for the colloidal fraction of four samples, and are essentially identical. Except for the ITA sample, the above observations suggest that dissolved Mo in Amazonian rivers is predominantly truly-dissolved, and that it is an increase in the size of this fraction that leads to higher dissolved concentrations in November. A previous study of Icelandic rivers (Pearce et al., 2010) also found that the contribution of the colloidal fraction to the dissolved total was small. Molybdenum isotope data for a limited number of colloidal fractions (Table S2), are not very different from the total dissolved load, with an average $\Delta^{98}Mo_{colloidal\text{-}dissolved} = -0.08 \pm 0.16$ (1SD) and a maximum of −0.31‰ for the Negro. This is in strong contrast to Icelandic rivers (Pearce et al., 2010) where $\Delta^{98}Mo_{colloidal\text{-}dissolved}$ is close to −1‰.

Molybdenum concentrations in Amazonian particulates are low: mostly in the range 0.2-0.5 ppm, with no significant difference between the residual fraction (HF-soluble fraction) and the bulk digest (Table S3). Black and clear water rivers represent a slight exception, with Tapajós and Negro particulates containing 0.6-1.2 ppm Mo. For the available Negro sample, the residual fraction contains only half the Mo of the total digest (0.56 versus 1.15 ppm). The fractions of Mo isolated from the particulate samples were all too small to obtain robust isotope analyses.

5. Discussion

5.1. Particulate-dissolved partitioning of soluble trace elements in the Amazon system

The data presented here re-emphasise the published finding (Archer and Vance, 2008; Pearce et al., 2010: Neubert et al., 2011; Voegelin et al., 2012; Rahaman et al., 2014; Wang et al., 2015; King and Pett-Ridge, 2018; Neely et al., 2018; Horan et al., 2020) that the heavy isotopes of Mo are preferentially partitioned into the dissolved load, relative to the upper continental crust (UCC, Fig. 3). As outlined in Fig. 3 and its caption, and taking account the new Amazon data, the global dissolved riverine load of Mo has an estimated δ^{98}Mo of about +0.8‰, compared to a recently proposed maximum for the UCC of +0.3‰ (Kendall et al., 2017). It is often suggested that such estimated global fluxes are biased to-

Table 1
Summary of the relative importance of the particulate and dissolved loads of Mo and Sr in Amazonian rivers.

Sample	Particulate Analysis[2]	Sr		Mo		Sr		Mo	
		Particulate/Dissolved[4]		Particulate/Dissolved		$F_{dissolved}$[5]		$F_{dissolved}$	
		In-situ[2]	Cosmogenic	In-situ	Cosmogenic	In-situ	Cosmogenic	In-situ	Cosmogenic
Solimões June[1]	res	0.13	0.26	0.08	0.15	0.88	0.79	0.93	0.87
Madeira June	res	0.37		0.28		0.73		0.78	
Negro June	res	0.01	0.03	0.11	0.40	0.99	0.97	0.90	0.71
Negro November	res	0.01	0.25	0.05	0.79	0.99	0.80	0.96	0.56
Trombetas June	res	0.00	0.02	0.00	0.23	1.00	0.98	1.00	0.81
Amazon Manaus June 55 m	res	0.02		0.01		0.98		0.99	
Amazon Óbidos June	total	0.10	0.46	0.04	0.18	0.91	0.69	0.96	0.85
Amazon Óbidos June 30 m	total	0.52		0.19		0.66		0.84	
Amazon Óbidos August	total	0.39		0.20		0.72		0.83	
Amazon Óbidos November	total	0.10		0.02		0.91		0.98	
Amazon Óbidos January	total	0.09		0.04		0.91		0.96	
Macapá South November	res	0.07		0.03		0.93		0.97	
Macapá North November	res	0.06		0.02		0.95		0.98	

[1] All particulate samples collected at 1 m depth, except where a depth is given.
[2] See Table S3 for data. "total" = bulk digest is used where available, "res" = the HF-soluble fraction where not. As seen from Table S3 there is generally no significant difference between the Mo concentrations in these analyses.
[3] Total particulate load from in-situ filtration. "Cosmogenic" based on long-term particulate load, where available (data from Wittmann et al., 2011).
[4] The ratio of the particulate to dissolved load carried by each river.
[5] The fraction of the total load (suspended + dissolved) that is contained in the dissolved fraction.

wards the Amazon (e.g. Miller et al., 2011), but this is not the case here. The Amazon represents 15-18% of the global riverine water discharge, and the next biggest rivers so far characterised for Mo (Chang Jiang and Ganges-Brahmaputra) have annual discharges 6-7 times lower. However, annual discharge-weighted Mo concentrations for the Amazon (at Óbidos) are 5-8 times lower than for the Chang Jiang and Ganges-Brahmaputra so that, in fact, all these rivers contribute sub-equally (about 5-10% each) to the global estimate of riverine Mo supply to the ocean. Moreover, these other large rivers have δ^{98}Mo values that are remarkably similar to the Amazon (+0.65 to +1.22: Archer and Vance, 2008; Neubert et al., 2011).

The data in the previous sections also highlight the degree to which the total Amazon Mo load is dominated by the dissolved phase (Table 1). This finding is consistent with early assessments of the marine budget of Mo (e.g. Morford and Emerson, 1999), but is rather different from other studies of both Mo (e.g. Pearce et al., 2010) and other elements (Viers et al., 2009; Jones et al., 2012; Jeandel and Oelkers, 2015). These latter studies have emphasised the potential importance of the suspended particulate load of rivers to oceanic budgets, assuming some mobilisation on continental margins. One significant and basic issue of importance to the marine budget of Mo and its isotopes is the degree to which our findings for the Amazon are typical of global rivers. In this section we first discuss the dissolved/particulate elemental partitioning of Mo.

Pearce et al. (2010) showed that the particulate Mo load in Icelandic rivers is slightly larger than the dissolved inventory. The bedload concentrations used by Pearce et al. (2010) for the suspended load, and the dissolved concentrations in these Icelandic rivers, are in the same range as those obtained here for the Amazon. The main difference is the size of suspended loads in Icelandic rivers, which are roughly an order of magnitude higher than for the Amazon main stem (Table S3). More generally, a number of studies have compared elemental inventories in the particulate and dissolved phase (<0.45 μm) of global rivers, also concluding that the suspended particulate inventory is greater for Mo, and other highly soluble elements, like Sr (e.g. Viers et al., 2009). This is, again, a very different picture from that obtained here, and in these cases the discrepancy appears to lie in differences in concentration data between studies. We illustrate this discrepancy here with Sr, in addition to Mo, because there are more Sr than Mo data available.

Three measured parameters go into the calculation of $R_{part/diss}$, the mass of the suspended particulate matter (SPM) per unit volume of water, the concentration of the element in question in SPM, and the dissolved concentration. With the exception of the black and clear water rivers (see below), the sizes of the SPM loads reported here are close to those reported previously for similar samples (Seyler and Boaventura, 2003; Bouchez et al., 2011). Table 1 calculates the suspended load as measured both on the particular sampling day via membrane filtration (in-situ) and the much longer-term average sediment flux obtained with cosmogenic nuclides (data from Wittmann et al., 2011). The SPM loads obtained here for the Madeira, as well as those for the Amazon main stem at Óbidos in the high-water season, are identical to those derived from cosmogenic data. The in-situ filtration SPM for the Solimões at Manacapuru is about half the cosmogenic value. The suspended particulate matter contents measured here for black and clear water rivers are anomalously low, but the dissolved load is still found to be important to dominant using the cosmogenic-derived estimates of SPM. In general, the $R_{part/diss}$ for Mo and Sr for our Amazon dataset (0.01-0.79 and 0.01-0.46, respectively), calculated using both of the above approaches to obtain SPM, are about an order of magnitude lower than the global values of 2.8 and 1.3 in the compilation of Viers et al. (2009).

The *dissolved* Mo and Sr concentrations obtained here are also very similar to those previously published for the Amazon (1.8-4.3 nM and 0.3 μM respectively: Gaillardet et al., 2005; Archer and Vance, 2008) and in compilations of global rivers (average 4.4 nM and 0.68 μM: Gaillardet et al., 2005). In fact, the main reason for the different conclusion regarding $R_{part/diss}$ lies in the elemental concentrations in SPM reported by different studies. The particulate Sr concentrations reported here are very close to those in another recent study of the Amazon (Bouchez et al., 2011). But the Viers et al. (2009) compilation tabulates particulate Sr concentrations for the Solimões that are up to a factor of 6 higher. These discrepancies for the Amazon would imply either that there is very significant temporal variability in particulate concentrations, which seems unlikely, or that there are technical problems with older data. This conclusion is similar to that we have recently arrived at for nickel (Ni), where particulate concentrations measured in our laboratory (Revels et al., 2021) and in Bouchez et al. (2011) are identical, but much lower than those in older publications that have been the basis of recent $R_{part/diss}$ comparisons.

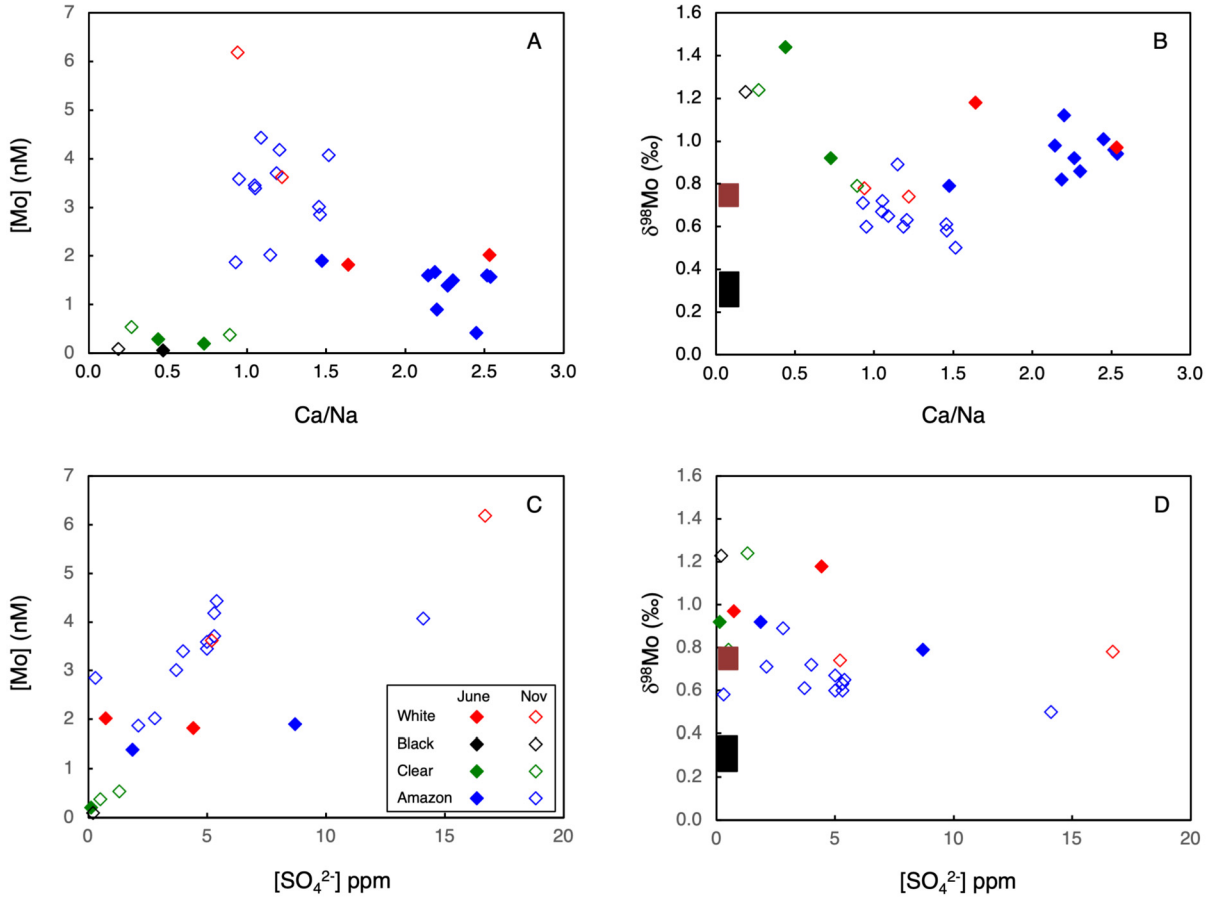

Fig. 4. Molybdenum concentrations (A, C) and Mo isotopes (B, D) of Amazon samples versus Ca/Na ratios and sulphate concentrations. Sulphate data presented here are supplemented by two analyses for June 2016 (Solimões at Manacapuru and Amazon at Óbidos) from the HYBAM dataset (https://hybam.obs-mip.fr/).

This discussion has significant implications for the relative importance of dissolved and suspended load transport in rivers. For example, for Mo and Sr data as reported here and in Bouchez et al. (2010, 2011), the dissolved load is dominant (60-100%). Even for relatively particulate-rich rivers like the Solimões and Madeira, 70-90% of the Mo and Sr is transported in the dissolved phase, consistent with Bouchez et al. (2010, 2011). We also note that for the particulate inventory to impact the dissolved marine budget it must be mobilised into solution from the solid phase. We find that essentially all Mo and about 60-90% of Sr in Amazon particulates is contained in a reservoir that is only mobilised in concentrated hydrofluoric acid, we assume in silicates. For this particulate reservoir to have any importance at all to the dissolved marine inventory, it would need to be much more easily mobilised in the oceans than in the laboratory. Finally, though there are hints at slightly more complicated behaviour in some, perhaps polluted, estuaries (e.g. Rahaman et al., 2014), mixing of riverine and seawater Mo and its isotopes in estuaries is close to conservative (Shiller and Boyle, 1991; Archer and Vance, 2008; Pearce et al., 2010), consistent with dissolved Mo being mostly "truly dissolved".

5.2. Minimal source control on Amazonian Mo and its isotopes

Chloride concentrations of Amazonian rivers are very low, with the highest dissolved chloride ion concentration measured here at 4.2 ppm, or 147 µM. Given molar Mo/Cl ratios in seawater of about 2×10^{-7}, the maximum sea-salt contribution to Amazonian dissolved Mo, via rainwater, amounts to about 0.02-0.03 nM. Though such a maximum possible contribution could, *in principle*, represent a significant portion of the Negro inventory of Mo, it is about two orders of magnitude lower than concentrations in most rivers. Miller et al. (2011) cite scarce published data for Mo concentrations in evaporitic minerals to dismiss evaporitic sources as significant for riverine Mo in general, also consistent with the high Mo/Cl rivers in Amazon rivers. Neither Mo concentrations nor isotope compositions correlate clearly with Ca/Na ratio (Fig. 4A, B), often used as an indicator of carbonate contributions to dissolved riverine loads. Carbonate Mo/Ca ratio of around 0.01-0.1 µmol/mol (Voegelin et al., 2009; Clarkson et al., 2020), in conjunction with measured Ca and Mo concentrations in Table 1, also imply negligible contributions from carbonate to dissolved loads of Mo.

Some previous studies have emphasised the potential importance of lithological and mineralogical sources of Mo and its isotopes in rivers (e.g. Neubert et al., 2011; Voegelin et al., 2012). In particular, Voegelin et al. (2012) suggest that the incongruent weathering of sulphide minerals may control the heavy Mo isotope composition. Moreover, Miller et al. (2011) use the linear relationship between Mo and SO_4^{2-} concentrations in global rivers to suggest that riverine Mo is predominantly sourced from pyrite weathering. We explore the issue of sulphide control on the dissolved loads of Amazonian rivers in Fig. 4 (though we only obtained SO_4^{2-} data for a subset of samples, nearly all low water season). There is clearly some relationship between Mo and SO_4^{2-} concentrations, but it is weaker than relationships between Mo concentrations and other parameters that have no link to sulphide, such as Na^+ or TZ^+ (Fig. 3). Furthermore, Mo isotope compositions are not correlated with SO_4^{2-}. While it is possible that the comparison of Mo isotopes and sulphate in Fig. 4D reflects different sources of sulphur (e.g., evaporitic sediment versus sulphide-rich sediment) with different Mo isotope compositions, Fig. 4D con-

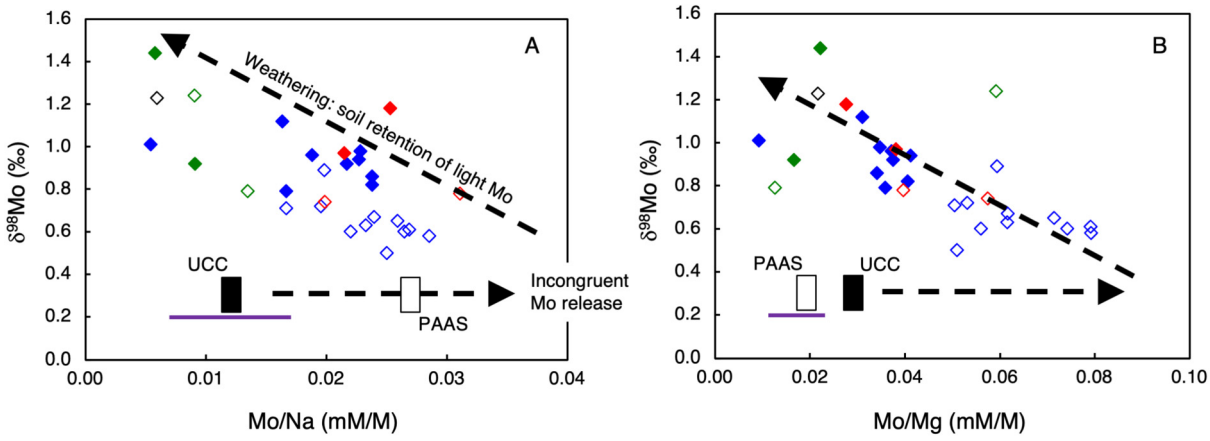

Fig. 5. Molybdenum isotope compositions of Amazonian rivers plotted against Mo/Na (A) and Mo/Mg (B). Mo/Na and Mo/Mg ratios for the upper continental crust (UCC) and Post-Archean Australian Shales (PAAS) are from McLennan (2001) and Taylor and McLennan (1985). The purple line shows the same ratios in particulate material from white rivers and the main Amazon stem. The dashed arrows are drawn to suggest that the data arrays for Amazonian rivers are consistent with the preferential retention of the light isotope of Mo in soils, but that the starting points of those arrays involve a source that is about three times enriched in Mo over both Na and Mg, relative to the UCC.

trasts with the systematic and consistent behaviour of Mo isotopes as a function of parameters unrelated to sulphate, such as [Na] and TZ^{+} seen in Fig. 3, and with Mo/Mg and Mo/Na ratios, discussed in the next section (Fig. 5). It may be that the relationships between the concentrations of all these elements, at least in the case of the Amazon Basin, do not generally reflect a common source but rather the fact that they all form highly soluble species in aqueous solution, as previously pointed out by Miller et al. (2011) for Mo, Re and sulphur.

5.3. Weathering controls on Amazon basin Mo and its isotopes

The interpretation of Mo isotopes in rivers as controlled by the incongruent weathering of isotopically heavy sulphide stands in contrast to an alternative view that emphasises the retention of light Mo in secondary minerals in the weathering environment (e.g. Archer and Vance, 2008; Pearce et al., 2010; Wang et al., 2015, 2018; Horan et al., 2020). An important argument for the control of Mo in rivers by pyrite weathering is that riverine Mo/S ratios are an order of magnitude below that of the UCC and closer to that of pyrite (Miller et al., 2011). These latter authors discuss the possibility that this difference could also be due to the absorptive loss of Mo to oxyhydroxides, but conclude that such loss cannot occur in the rivers themselves because of their already low Mo/S ratios. We argue below that absorptive loss of light Mo from the aqueous phase *in soils*, before the Mo enters the rivers, is crucial for riverine isotope compositions. This is consistent with other published studies (Archer and Vance, 2008; Pearce et al., 2010; Wang et al., 2015, 2018; Horan et al., 2020) and with recent findings of light Mo in secondary minerals and organic matter in soils (e.g. Siebert et al., 2015; King et al., 2016, 2018; Wang et al., 2018).

Following Dellinger et al. (2015), Revels et al. (2021) used element/Na and element/Mg ratios as a tracer for Ni depletion in the dissolved phase as a result of secondary mineral precipitation. We take this approach again for Mo in Fig. 5. Though there is certainly more scatter in the Mo data than for either Li or Ni, the data arrays for rivers in Fig. 5 are consistent with preferential retention of Mo over both Na and Mg coupled to an isotope fractionation. There is one significant difference, however, between the behaviour of Mo and Li. For Li, the lower end of the array is close to estimates of the source rock composition for Li and its isotopes (Dellinger et al., 2015). There are insufficient data on Mo in Amazonian rocks and river sediments to be unequivocal, but it appears that the starting point of the arrays for Mo at isotope compositions close to the UCC have Mo/Na and Mo/Mg ratios that are both about a factor of three to four higher than the UCC. This could be explained by enrichment in Mo in Amazonian source rocks relative to the UCC given, for example, the predominance of sedimentary rocks (including shales) in Andean catchments (e.g., Dellinger et al., 2015). Fig. 5 also shows Mo/Na and Mo/Mg ratios for Post-Archean Australian Shales (PAAS; Taylor and McLennan, 1985), also displaced from the lower end of the arrays though less so for Mo/Na. Finally, Mo/Na and Mo/Mg of particulate samples in the white water rivers and main stem Amazon (Table S3) are also not very different from the UCC (Fig. 5).

The above discussion suggests that the high Mo/Na and Mo/Mg of Amazonian rivers may not be due to an overall enrichment of Mo in the rocks of Amazonian river catchments. It could also be that the high Mo/Na and Mo/Mg ratios of Amazon rivers is due to incongruent release from a Mo-enriched mineralogical source such as pyrite, as suggested by Miller et al. (2011). If that is the case, the average isotope composition of that Mo would need to be the same as the UCC and the same for all river catchments, in order to keep the coherence of the arrays on Fig. 5. Overall, then, the Amazon data are best-explained by (a) Mo enrichment over the UCC in the dissolved phase, to a broadly similar extent in all rivers, of about factor 3 relative to Na and Mg, due to preferential release of Mo from the source material, but followed by; (b) partial retention of Mo in soils, with preferential retention of the light isotope, as the main control on coupled Mo-δ^{98}Mo systematics.

The pattern for Mo shows an additional significant difference versus Li and Ni. For both Li and Ni (Dellinger et al., 2015; Revels et al., 2021), the black and clear water rivers tend to lie closer to the UCC on the equivalent plots to Fig. 5 here. For Li this finding has been attributed to high weathering intensities, leading to more quantitative mobilisation from the solid phase and thus greater dissolution of previously precipitated oxides and clay minerals in acidic soil environments, releasing light Li (Dellinger et al., 2015). But for Mo, the black and clear water samples lie at the other end of the trends on Fig. 5, furthest away from the UCC in Mo/Na, Mo/Mg ratios and δ^{98}Mo. Molybdenum also shows an opposite relationship to pH versus Ni (Fig. 6): low pH is associated with low Mo concentrations, and isotope compositions that are furthest from the UCC. In this context it is interesting to note that Mo adsorption to surfaces increases at low pH (e.g. King et al., 2018). We speculate that lower pH favours the continued retention of Mo in soils through sorption to available mineral and organic matter surfaces, while other elements are exported to the aqueous phase. This is further supported by the fact that particulate Mo/Na and Mo/Mg ratios for these black and clear water rivers are a factor

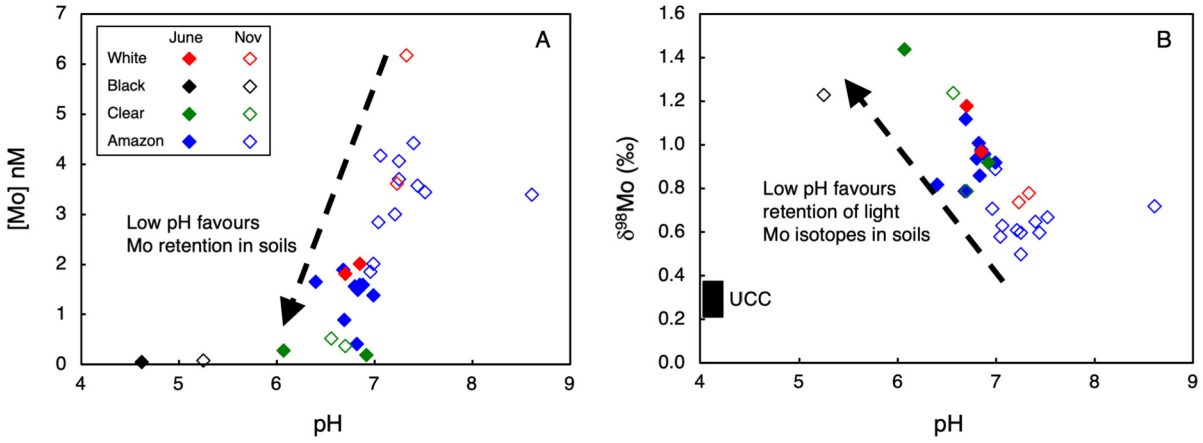

Fig. 6. Molybdenum concentrations (A) and isotope compositions (B) of Amazonian rivers plotted against pH.

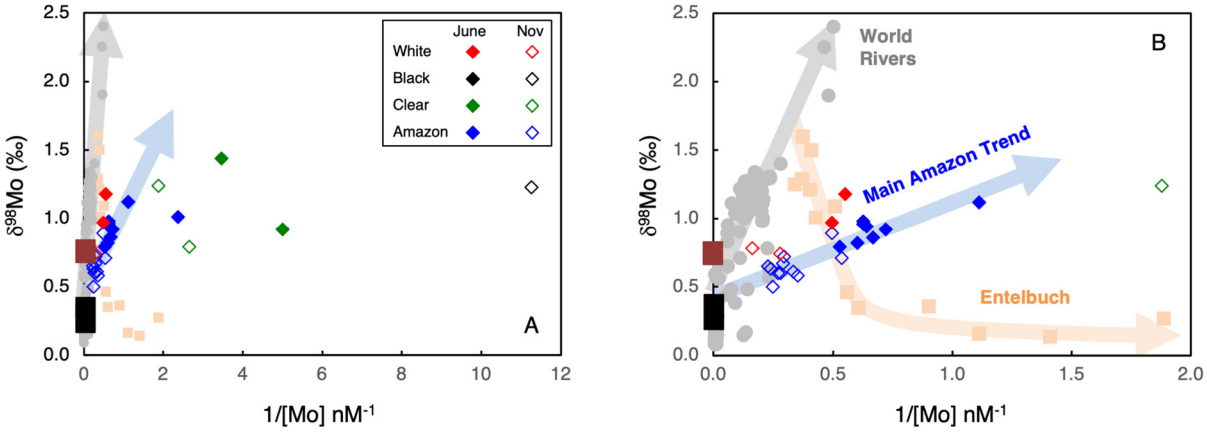

Fig. 7. Molybdenum isotope compositions of Amazonian rivers plotted versus 1/Mo and compared with selected data from the literature. Panel B is simply an enlargement of panel A, in order to show some of the detail at higher Mo concentrations. Most of the "world rivers" data come from Archer and Vance (2008), including samples from the Amazon, the Chang Jiang, the Brahmaputra, the St. Lawrence catchment, the Nile and the Kalix (Sweden). It also includes data from rivers in Sikkim, the Chang Jiang, and the Aare catchment (Switzerland) in Neubert et al. (2011), and from the Xijiang and Huanghe rivers in China (Wang et al., 2015). The Entlebuch catchment data (Switzerland) are also from Neubert et al. (2011).

of 10-30 greater than for white water rivers (data in Table S3). Finally, for all Amazon rivers, the low water season (November) samples contain more Mo with a lower δ^{98}Mo and have the highest measured pH.

5.4. Global context: the control of weathering regime on riverine Mo isotopes

Archer and Vance (2008) interpreted riverine δ^{98}Mo data in terms of relationships with 1/Mo. These authors rationalised the array labelled "world rivers" on Fig. 7 in terms of variable retention of the light isotope in particulate material and preferential release of the heavy isotope to the dissolved phase. The new data for the main Amazon stem show qualitatively similar behaviour to the previously published data, but the trend is flatter (Fig. 7). The new data lead us to hypothesise that the precise behaviour pattern of variation of Mo and its isotopes relates to weathering rate and intensity in the catchment(s) concerned. Most of the data that define the "world rivers" array on Fig. 7 derive from catchments where chemical weathering is rapid but incomplete, or low intensity, so that there is capacity to retain isotopically light Mo in secondary minerals in soils. This main group of rivers include those that drain mountain belts in their upper reaches (including the Chang Jiang, Xijiang and Huanghe in China, the Brahmaputra, a small river in Sikkim, and the Aare in Switzerland: see caption to Fig. 7 for data sources), where physical denudation produces substrate faster than chemical weathering can operate. It also includes catchments where weathering is likely to be low intensity for climatic reasons, such as the Kalix in Sweden and the St. Lawrence catchment in Canada. Data for the Nile lie close to the same trend but slightly below it (Archer and Vance, 2008).

We hypothesise that the new data for the Amazon Basin show a qualitatively similar pattern because the same general control operates – the retention of light Mo in soils. We further suggest that the slope of the data array is lower in the Amazon because of higher weathering intensity leading, overall, to less extreme δ^{98}Mo for a given Mo concentration because of weaker retention of light Mo in soils. This suggestion is supported by the fact that data for different Amazon river types lie off the main Amazon trend in Fig. 7 in a systematic way: data for white rivers lie slightly above it, closer to that for "world rivers", while those for lowland black and clear rivers lie significantly below it, at lower Mo concentrations for a given δ^{98}Mo. The hypothesis that these data arrays are controlled by rate and intensity of weathering, itself a function of the tectonic and climatic regime in the catchment, finds further support in data from other recent publications. Fig. 8A, for example, shows data for Hawaiian rivers and groundwater (King and Pett-Ridge, 2018) which, in general, shows similar characteristics to the lowland rivers of the Amazon but is flatter still, consistent with the intense tropical weathering of basalt in this regime, and the fact that even young soils on Hawaii are already extremely depleted in base cations (e.g., Vance et al., 2016). At the other ex-

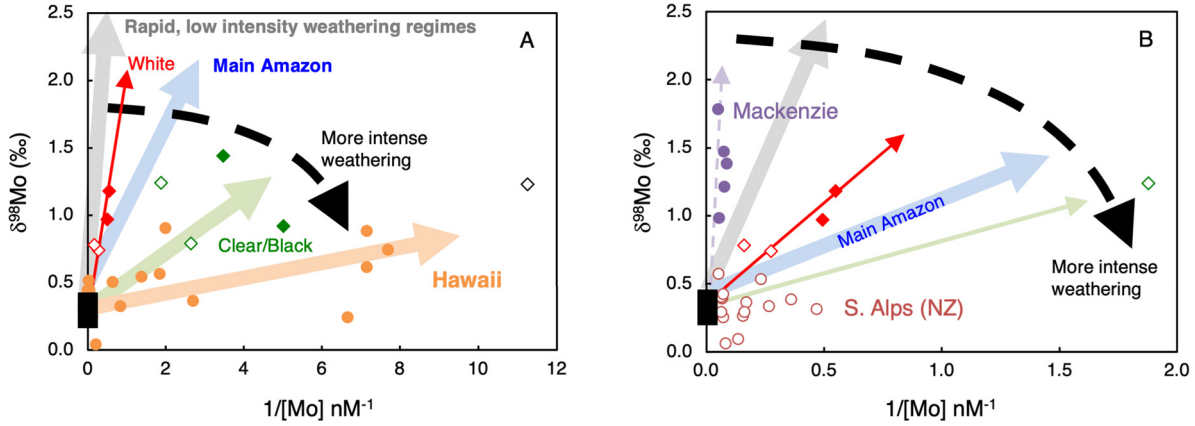

Fig. 8. Mo-δ^{98}Mo trends in Amazonian and global rivers compared to other published datasets for (A) Hawaiian rivers and groundwaters (King and Pett-Ridge, 2018) and (B) rivers in the Southern Alps of New Zealand and the Mackenzie (Horan et al., 2020). Note the different scales for the x-axes in A and B. The colour-coding of the arrows in B, where not labelled, is the same as for A. All these riverine data, taken as a whole and with the exception of those for the Southern Alps of New Zealand, suggest reasonably systematic relationships for sets of rivers with similar weathering regime in terms of the rate and intensity of weathering, and a systematic progression towards lower slopes on this diagram as weathering intensity increases. See text for further discussion.

treme, the data for the Mackenzie River in Arctic Canada (Horan et al., 2020) lie on the steepest array of all. These data come from a setting that is partially high altitude and partially glaciated, leading to high physical weathering rates. Perhaps more significantly, the Mackenzie catchment is also a setting in which low temperatures and permafrost lead to low chemical weathering intensities.

On the other hand, other recent data for the Southern Alps of New Zealand (Horan et al., 2020), another high altitude, low temperature setting where physical weathering is likely to be relatively more important than chemical weathering, are harder to explain in the context of this framework (Fig. 8B). The data from a small catchment in Switzerland, the Entlebuch catchment (Fig. 7: Neubert et al., 2011) represents another interesting deviation. Indeed, the Entlebuch data look quite different from those for the adjacent Aare catchment, which conform to the "world river" array on Fig. 7, in the same study. The original paper interpreted these differences in terms of catchment lithology (Neubert et al., 2011). We suggest that, while lithology must have some impact, it is also significant that the tributaries of both the Aare and the Entlebuch, which lie above the Amazon trend, drain tectonically complex, high altitude terrains. On the other hand, the tributaries lying on the gentle part of the Entlebuch trend, at lower and relatively constant δ^{98}Mo, drain agricultural land. Furthermore, this part of the catchment is underlain by continental sediments that have seen a previous weathering cycle in a significantly more tropical climatic setting than the current one.

6. Summary and conclusions

The data presented in this paper demonstrate that the dissolved load of the Amazon is the most important vector for delivery of Mo to the oceans and that this finding is common to other highly soluble elements like Sr. This assessment of the relative importance of the riverine dissolved and particulate loads for these elements is different from published studies, which have emphasised the importance of the particulate load. In common with studies of other rivers, the dissolved load of the Amazon is heavier than the upper continental crust. The new data suggest that the global riverine flux of Mo has a δ^{98}Mo of about $+0.8‰$ versus the value for the UCC of about $+0.3‰$. We stress that this value is not dominated by the Amazon data: though the water discharge of the Amazon is much greater than all other rivers, Mo concentrations are lower. We attribute the heavy dissolved load of rivers to preferential retention of light Mo in soils.

A compilation of published data and a comparison with the new data presented here for the Amazon reveals patterns of variation of Mo and its isotopes in rivers that are most easily explained in terms of the chemical weathering regime. While we suggest that the same general process operates in all catchments, retention of isotopically light Mo in soils, its impact is a function of weathering intensity. When physical weathering rates are high relative to chemical weathering rates, in other words where weathering intensity is low, rivers can develop very high δ^{98}Mo for a given Mo concentration. In contrast, when weathering intensities are high, δ^{98}Mo of rivers is significantly closer to the rocks of the upper continental crust. This finding has important consequences for semi-quantitative applications of Mo isotopes to the history of oceanic redox, because it suggests that both tectonics and climate will control the riverine input that is partitioned between different redox-controlled oceanic sinks. For example, with its cold climate and high mountains, the Cenozoic would see low weathering intensities and a heavy riverine flux to the oceans. On the other hand, the Mo isotope input flux relevant to the greenhouse conditions and quiescent tectonics of the Mesozoic, including the Oceanic Anoxic Events that the Mo isotope redox tool has been extensively applied, would be significantly closer to the upper continental crust.

CRediT authorship contribution statement

Vance: Conceptualization, Methodology, Original draft preparation. **Revels:** Fieldwork, Analysis, Original draft preparation. **Rickli:** Fieldwork, Reviewing and editing. **Moura:** Fieldwork and sample collection.

Declaration of competing interest

The authors declare that they have no known competing financial interests or personal relationships that could have appeared to influence the work reported in this paper.

Acknowledgements

This research was supported by the ETH Zürich (Grant ETH-06 14-1) and the Swiss National Science Foundation (Grant 200020_165904). The authors are grateful for very efficient editorial handling by Fred Moynier, and for insightful comments by Julien Bouchez and an anonymous reviewer.

Appendix A. Supplementary material

Supplementary material related to this article can be found online at https://doi.org/10.1016/j.epsl.2021.116773.

References

Allard, T., et al., 2011. Tracing source and evolution of suspended particles in the Rio Negro basin (Brazil) using chemical species of iron. Chem. Geol. 280, 79–88.

Archer, C., Vance, D., 2008. The global riverine Mo isotope flux and quantitative estimates of anoxia in the ancient global ocean. Nat. Geosci. 1, 597–600.

Arnold, G.L., Anbar, A.D., Barling, J., Lyons, T.W., 2004. Molybdenum isotope evidence for widespread anoxia in Mid-Proterozoic oceans. Science 304, 87–89.

Barling, J., Anbar, A.D., 2004. Molybdenum isotope fractionation during adsorption by manganese oxides. Earth Planet. Sci. Lett. 217, 315–329.

Bouchez, J., et al., 2010. Turbulent mixing in the Amazon River: the isotopic memory of confluences. Earth Planet. Sci. Lett. 290, 37–43.

Bouchez, J., Gaillardet, J., France-Lanord, C., Maurice, L., Dutra-Maia, P., 2011. Grain size control on river suspended sediment geochemistry: clues from Amazon River depth profiles. Geochem. Geophys. Geosyst. 12. https://doi.org/10.1029/2010GC003380.

Bura-Nakić, E., Andersen, M.B., Archer, C., de Souza, G.F., Marguš, M., Vance, D., 2018. Coupled Mo-U abundances and isotopes in a small marine euxinic basin: constraints on processes in euxinic basins. Geochim. Cosmochim. Acta 222, 212–229.

Callède, J., Cochonneau, G., Vieira Alves, F., Guyot, J.-L., Guimarães, S., De Oliveira, E., 2010. Les apports en eau de l'Amazone à l'Océan Atlantique. Rev. Sci. Eau 23, 247–273.

Clarkson, M.O., Müsing, K., Andersen, M.B., Vance, D., 2020. Examining pelagic carbonate-rich sediments as an archive for authigenic uranium and molybdenum isotopes using reductive cleaning and leaching experiments. Chem. Geol. 539, 119412.

Dellinger, M., et al., 2015. Riverine Li isotope fractionation in the Amazon River basin controlled by the weathering regimes. Geochim. Cosmochim. Acta 164, 71–93.

Fittkau, E.J., Ilmer, U., Junk, W.K., Reiss, F., Schmidt, G.W., 1975. Productivity Biomass, and Population Dynamics of the Amazonian Water Bodies. Springer-Verlag, New York.

Fritsch, E., et al., 2011. Deciphering the weathering processes using environmental mineralogy and geochemistry: towards an integrated model of laterite and podzol genesis in the upper Amazon basin. C. R. Géosci. 343, 188–198.

Gaillardet, J., Dupré, B., Allègre, C., Négrel, P., 1997. Chemical and physical denudation in the Amazon River basin. Chem. Geol. 142, 141–173.

Gaillardet, J., Viers, J., Dupré, B., 2005. Trace elements in river waters. In: Treatise on Geochemistry, vol. 5, pp. 225–272.

Gibbs, R.J., 1967. Amazon River: environmental factors that controls its suspended load. Science 156, 1734–1737.

Gibbs, R.J., 1977. Transport phases of transition metals in the Amazon and Yukon rivers. Geol. Soc. Am. Bull. 88, 829–843.

Helz, G., et al., 1996. Mechanism of molybdenum removal from the sea and its concentration in black shales: EXAFS evidence. Geochim. Cosmochim. Acta 60, 3631–3642.

Horan, K., et al., 2020. Unravelling the controls on the molybdenum isotope ratios of river waters. Geochem. Perspect. Lett. 13, 1–6.

Jeandel, C., Oelkers, E.H., 2015. The influence of terrigenous particulate material dissolution on ocean chemistry and global element cycles. Chem. Geol. 395, 50–66.

Jones, M.T., Pearce, C.R., Oelkers, E.H., 2012. An experimental study of the interaction of basaltic riverine particulate material and seawater. Geochim. Cosmochim. Acta 77, 108–120.

Kendall, B., Dahl, T.W., Anbar, A.D., 2017. The stable isotope geochemistry of molybdenum. Rev. Mineral. Geochem. 82, 683–732.

King, E.E., Thompson, A., Chadwick, O.A., Pett-Ridge, J.C., 2016. Molybdenum sources and isotopic composition during early stages of pedogenesis along a basaltic climate transect. Chem. Geol. 445, 54–67.

King, E.E., Pett-Ridge, J.C., 2018. Reassessing the dissolved molybdenum isotopic composition of ocean inputs: the effect of chemical weathering and groundwater. Geology 46, 955–958.

King, E.E., Perakis, S.S., Pett-Ridge, J.C., 2018. Molybdenum isotope fractionation during adsorption to organic matter. Geochim. Cosmochim. Acta 222, 584–598.

Konhauser, K.O., Fyfe, W.S., Kronberg, B.I., 1994. Multi-element chemistry of some Amazonian waters and soils. Chem. Geol. 111, 155–175.

McLennan, S.M., 2001. Relationships between the trace element compositions of sedimentary rocks and upper continental crust. Geochem. Geophys. Geosyst. 2, 2000GC000109.

Miller, C.A., Peucker-Ehrenbrink, B., Walker, B.D., Marcantonio, F., 2011. Re-assessing the surface cycling of molybdenum and rhenium. Geochim. Cosmochim. Acta 75, 7146–7179.

Morford, J.L., Emerson, S., 1999. The geochemistry of redox sensitive trace metals in sediments. Geochim. Cosmochim. Acta 63, 1735–1750.

Nägler, T.F., Siebert, C., Lüschen, H., Böttcher, M.E., 2005. Sedimentary Mo isotope record across the Holocene fresh–brackish water transition of the Black Sea. Chem. Geol. 219, 283–295.

Nägler, T.F., et al., 2014. Proposal for an international molybdenum isotope measurement standard and data representation. Geostand. Geoanal. Res. 38, 149–151.

Nakagawa, Y., et al., 2012. The molybdenum isotopic composition of the modern ocean. Geochem. J. 46, 131–141.

Neely, R.A., et al., 2018. Molybdenum isotope behaviour in groundwaters in terrestrial hydrothermal systems, Iceland. Earth Planet. Sci. Lett. 486, 108–118.

Neubert, N., Nägler, T.F., Böttcher, M.E., 2008. Sulfidity controls molybdenum isotope fractionation into euxinic sediments: evidence from the modern Black Sea. Geology 36, 775–778.

Neubert, N., et al., 2011. The molybdenum isotopic composition in river water: constraints from small catchments. Earth Planet. Sci. Lett. 304, 180–190.

Oelkers, E.H., Gislason, S.R., Eiriksdottir, E.S., Jones, M., Pearce, C.R., Jeandel, C., 2011. The role of riverine particulate material on the global cycles of the elements. Appl. Geochem. 26, S365–S369.

Pearce, C.R., et al., 2010. Molybdenum isotope behaviour accompanying weathering and riverine transport in a basaltic terrain. Earth Planet. Sci. Lett. 295, 1–4–1-114.

Poulson Brucker, R.L., McManus, J., Severmann, S., Berelson, W.M., 2009. Molybdenum behavior during early diagenesis: insights from Mo isotopes. Geochem. Geophys. Geosyst. 10.

Rahaman, W., Goswami, V., Singh, S.K., Rai, V.K., 2014. Molybdenum isotopes in two Indian estuaries: mixing characteristics and input to the oceans. Geochim. Cosmochim. Acta 141, 407–422.

Revels, B.N., Rickli, J., Moura, C.A.V., Vance, D., 2021. Nickel and its isotopes in the Amazon basin: the impact of weathering regime and delivery to the ocean. Geochim. Cosmochim. Acta 293, 344–364.

Seyler, P.T., Boaventura, G.R., 2003. Distribution and partition of trace metals in the Amazon basin. Hydrol. Process. 7, 1345–1361.

Siebert, C., Nägler, T.F., von Blanckenburg, F., Kramers, J.D., 2003. Molybdenum isotope records as a potential new proxy for paleoceanography. Earth Planet. Sci. Lett. 211, 159–171.

Siebert, C., McManus, J., Bice, A., Poulson, R., Berelson, W.M., 2006. Molybdenum isotope signatures in continental margin marine sediments. Earth Planet. Sci. Lett. 241, 723–733.

Siebert, C., et al., 2015. Molybdenum isotope fractionation in soils: influence of redox conditions, organic matter, and atmospheric inputs. Geochim. Cosmochim. Acta 162, 1–24.

Shiller, A.M., Boyle, E.A., 1991. Trace elements in the Mississippi River delta outflow region: behavior at high discharge. Geochim. Cosmochim. Acta 55, 3241–3251.

Stallard, R.F., Edmond, J.M., 1983. Geochemistry of the Amazon, 2: the influence of geology and weathering environment on the dissolved load. J. Geophys. Res. 88C, 9671–9688.

Taylor, S.R., McLennan, S.M., 1985. The Continental Crust: Its Composition and Evolution. Blackwell, Malden, Mass.

Vance, D., et al., 2016. The behaviour of Cu and Zn isotopes during soil development: controls on the dissolved load of rivers. Chem. Geol. 445, 36–53.

Viers, J., Dupré, B., Gaillardet, J., 2009. Chemical composition of suspended sediments in world rivers: new insights from a new database. Sci. Total Environ. 407, 853–868.

Voegelin, A.R., Nägler, T.F., Samankassou, E., Villa, I.M., 2009. Molybdenum isotope compositions of modern and Carboniferous sediments. Chem. Geol. 265, 488–498.

Voegelin, A.R., et al., 2012. The impact of igneous bedrock weathering on the Mo isotopic composition of stream waters: natural samples and laboratory experiments. Geochim. Cosmochim. Acta 86, 150–165.

Wasylenki, L.E., Rolfe, B.A., Weeks, C.L., Spiro, T.G., Anbar, A.D., 2008. Experimental investigation of the effects of temperature and ionic strength on Mo isotope fractionation during adsorption to manganese oxides. Geochim. Cosmochim. Acta 72, 5997–6005.

Wang, A., et al., 2015. Chemical weathering controls on variations in the molybdenum isotopic composition of river water: evidence from large rivers in China. Chem. Geol. 410, 201–212.

Wang, A., et al., 2018. Fe (hydro) oxide controls Mo isotope fractionation during the weathering of granite. Geochim. Cosmochim. Acta 226, 1–17.

West, A., Galy, A., Bickle, M., 2005. Tectonic and climatic controls on silicate weathering. Earth Planet. Sci. Lett. 235, 211–228.

Wittmann, H., von Blanckenburg, F., Maurice, L., Guyot, J.-L., Filizola, N., Kubik, P.W., 2011. Sediment production and delivery in the Amazon River basin quantified by in-situ produced cosmogenic nuclides and recent river loads. Geol. Soc. Am. Bull. 123, 934–950.